data showed a decay of 5% and a variation of ±2% over the period of data collection; hence, an appropriate correction was applied. Of the 6129 intensity data collected, 5675 unique observations remained after averaging of duplicate and equivalent measurements and deletion of systematic absences, all of which were retained for use in structure solution and refinement. The absorption correction was applied on the basis of the indexed crystal faces, maximum and minimum transmission coefficients being 0.459 and 0.364, respectively. Lorentz and polarization corrections were applied. Structure solution was by conventional heavy-atom (Patterson and difference Fourier) methods and refinement by blocked-cascade full-matrix least squares. Weights w were set equal to $[\sigma_c^2(F_o) + gF_o^2]^{-1}$, where $\sigma_c^2(F_o)$ is the variance in F_o due to counting statistics and $g = 0.0005$ was chosen to minimize the variation in S as a function of $|F_o|$. All non-hydrogen atoms were assigned anisotropic displacement parameters, and all hydrogen atoms, fixed isotropic displacement parameters. All non-hydrogen atoms and the hydrogen atom H(1) were refined without positional constraints. All other hydrogen atoms were constrained to idealized geometries (C–H = 0.96 Å, H–C–H = 109.5°). Final difference electron density maps showed no features outside the range +1.3 to −1.3 e Å^{-3}, the largest of these being close to the lutetium atom. One ethyl group [C(36), C(37a), and C(37b)] showed a two-site disorder, with the methyl carbons well separated and refined as two distinct atomic sites [C(37a) and C(37b)] of occupancy 0.53 (2) and 0.47 (2), respectively. The methylene group [C(36)] was refined as a single atomic site, with some consequent distortion of the apparent geometry around this atom. Residuals at convergence are listed in Table I. All calculations were carried out with Nicolet proprietary software using complex neutral-atom scattering factors taken from ref 50.

Acknowledgment. We thank Prof. Dr. J. W. Buchler (Technische Hochschule, Darmstadt, Germany) for some useful comments.

Supplementary Material Available: Complete tables of data collection parameters, bond distances and angles, anisotropic thermal parameters, and hydrogen atomic coordinates for **1a** (6 pages); a table of observed and calculated structure factor amplitudes for **1a** (21 pages). Ordering information is given on any current masthead page.

Contribution from the Department of Inorganic and Physical Chemistry,
Indian Institute of Science, Bangalore 560 012, India

Reactivity of PPh_3 toward $Ru^{II}Ru^{III}Cl(O_2CAr)_4$: Syntheses, Molecular Structures, and Spectroscopic and Electrochemical Properties of $Ru^{II}Ru^{III}(OH_2)Cl(MeCN)(O_2CAr)_4(PPh_3)_2$ and $Ru^{II}_2(OH_2)(MeCN)_2(O_2CAr)_4(PPh_3)_2$

Birinchi K. Das and Akhil R. Chakravarty*

Received December 17, 1990

By the reaction of $Ru_2Cl(O_2CAr)_4$ (**1**) and PPh_3 in MeCN–H_2O the diruthenium(II,III) and diruthenium(II) compounds of the type $Ru_2(OH_2)Cl(MeCN)(O_2CAr)_4(PPh_3)_2$ (**2**) and $Ru_2(OH_2)(MeCN)_2(O_2CAr)_4(PPh_3)_2$ (**3**) were prepared and characterized by analytical, spectral, and electrochemical data (Ar is an aryl group, C_6H_4-*p*-X; X = H, OMe, Me, Cl, NO_2). The molecular structure of $Ru_2(OH_2)Cl(MeCN)(O_2CC_6H_4\text{-}p\text{-}OMe)_4(PPh_3)_2$ was determined by X-ray crystallography. Crystal data are as follows: triclinic, $P\bar{1}$, $a = 13.538$ (5) Å, $b = 15.650$ (4) Å, $c = 18.287$ (7) Å, $\alpha = 101.39$ (3)°, $\beta = 105.99$ (4)°, $\gamma = 97.94$ (3)°, $V = 3574$ Å^3, $Z = 2$. The molecule is asymmetric, and the two ruthenium centers are clearly distinguishable. The Ru^{III}–Ru^{II}, Ru^{III}–(μ-OH_2), and Ru^{II}–(μ-OH_2) distances and the Ru–(μ-OH_2)–Ru angle in $[\{Ru^{III}Cl(\eta^1\text{-}O_2CC_6H_4\text{-}p\text{-}OMe)(PPh_3)\}(\mu\text{-}OH_2)(\mu\text{-}O_2CC_6H_4\text{-}p\text{-}OMe)_2\{Ru^{II}(MeCN)(\eta^1\text{-}O_2CC_6H_4\text{-}p\text{-}OMe)(PPh_3)\}]$ are 3.604 (1), 2.127 (8), and 2.141 (10) Å and 115.2 (5)°, respectively. The compounds are paramagnetic and exhibit axial EPR spectra in the polycrystalline form. An intervalence transfer (IT) transition is observed in the range 900–960 nm in chloroform in these class II type trapped mixed-valence species **2**. Compound **2** displays metal-centered one-electron reduction and oxidation processes near −0.4 and +0.6 V (vs SCE), respectively in CH_2Cl_2–TBAP. Compound **2** is unstable in solution phase and disproportionates to (μ-aquo)diruthenium(II) and (μ-oxo)diruthenium(III) complexes. The mechanistic aspects of the core conversion are discussed. The molecular structure of a diruthenium(II) compound, $Ru_2(OH_2)(MeCN)_2(O_2CC_6H_4\text{-}p\text{-}NO_2)_4(PPh_3)_2\cdot 1.5CH_2Cl_2$, was obtained by X-ray crystallography. The compound crystallizes in the space group $P2_1/c$ with $a = 23.472$ (6) Å, $b = 14.303$ (3) Å, $c = 23.256$ (7) Å, $\beta = 101.69$ (2)°, $V = 7645$ Å^3, and $Z = 4$. The Ru^{II}–Ru^{II} and two Ru^{II}–(μ-OH_2) distances and the Ru^{II}–(μ-OH_2)–Ru^{II} angle in $[\{(PPh_3)(MeCN)(\eta^1\text{-}O_2CC_6H_4\text{-}p\text{-}NO_2)Ru\}_2(\mu\text{-}OH_2)(\mu\text{-}O_2CC_6H_4\text{-}p\text{-}NO_2)_2]$ are 3.712 (1), 2.173 (9), and 2.162 (9) Å and 117.8 (4)°, respectively. In both diruthenium(II,III) and diruthenium(II) compounds, each metal center has three facial ligands of varying π-acidity and the aquo bridges are strongly hydrogen bonded with the η^1-carboxylato facial ligands. The diruthenium(II) compounds are diamagnetic and exhibit characteristic ^1H NMR spectra in $CDCl_3$. These compounds display two metal-centered one-electron oxidations near +0.3 and +1.0 V (vs SCE) in CH_2Cl_2–TBAP. The overall reaction between **1** and PPh_3 in MeCN–H_2O through the intermediacy of **2** is of the disproportionation type. The significant role of facial as well as bridging ligands in stabilizing the core structures is observed from electrochemical studies.

Introduction

An interesting aspect of the chemistry of metal–metal multiple-bonded tetracarboxylates is the reactivity of monodentate tertiary phosphines toward the dimetallic cores.[1,2] The usual mode of bonding of the phosphine ligand is axial and/or equatorial with respect to the dimeric core. In these substitution type reactions, the M–M bond order of the core remains unaltered when the dimeric unit is not cleaved. Triarylphosphines are also known[3] to act as three-atom bridging ligands on orthometalation to one aryl group.

Earlier attempts to prepare axially coordinated PPh_3 complexes of ruthenium of the type $[Ru_2(O_2CR)_4(PPh_3)_2]^+$ led to the formation of oxo-bridged diruthenium and triruthenium complexes.[4,5] The reactivity of the diruthenium core is of interest since the dimeric rhodium(II) carboxylates with a similar core structure are known to form stable axial adducts with P- and N-donor ligands.[1,6] The unusual reactivity of the $\{Ru_2(O_2CR)_4^+\}$ core could be due to the stability of its $\sigma^2\pi^4\delta^2(\delta^*\pi^*)^3$ ground electronic

---

(1) Cotton, F. A.; Walton, R. A. *Multiple Bonds Between Metal Atoms*; John Wiley & Sons: New York, 1982.

(2) Cotton, F. A.; Walton, R. A. *Struct. Bonding* (*Berlin*) **1985**, *62*, 1.

(3) Chakravarty, A. R.; Cotton, F. A.; Tocher, D. A. *Inorg. Chem.* **1984**, *23*, 4697. Chakravarty, A. R.; Cotton, F. A.; Tocher, D. A.; Tocher, J. H. *Organometallics* **1985**, *4*, 8.

(4) Schröder, M.; Stephenson, T. A. In *Comprehensive Coordination Chemistry*; Wilkinson, G., Gillard, R. D., McCleverty, J. A., Eds.; Pergamon Press: Oxford, England, 1987; Vol. 4, pp 277–518.

(5) Legzdins, P.; Mitchell, R. W.; Rempel, G. L.; Ruddick, J. D.; Wilkinson, G. *J. Chem. Soc., A* **1970**, 3322. Cotton, F. A.; Norman, J. G., Jr. *Inorg. Chim. Acta* **1972**, *6*, 411.

(6) Jardine, F. H.; Sheridan, P. S. In *Comprehensive Coordination Chemistry*; Wilkinson, G., Gillard, R. D., McCleverty, J. A., Eds.; Pergamon Press: Oxford, England, 1987; Vol. 4, pp 901–1096.

0020-1669/91/1330-4978$02.50/0

configuration.[7] It is known that the reaction between PPh_3 and $Ru_2Cl(ArCONH)_4$ leads[8] to the formation of an edge-sharing bioctahedral complex, $Ru_2(Ph)_2(ArCONH)_2[Ph_2POC(Ar)N]_2$, with an Ru–Ru bond order of 1.0. The reaction involves a transfer of one phenyl group from PPh_3 on to the metal center along with a synergic transfer of the bridging amido oxygen to the phosphorus atom. The present work stems from our interest to explore the reactivity of PPh_3 toward the tetrabis(arenecarboxylato)diruthenium(II,III) core in the precursor $Ru_2Cl(\mu\text{-}O_2CAr)_4$, which is structurally similar to the tetraamidato species. Earlier studies have shown that PPh_3 reacts with $Ru_2Cl(O_2CMe)_4$ in MeOH to form only $Ru_2O(O_2CMe)_4(PPh_3)_2$.[9] On reinvestigation of the reaction with excess PPh_3 in an alcoholic medium ($R'CH_2OH$), the products isolated are monomeric ruthenium(II) compounds containing carbonyl ligands.[10] Using $Ru_2Cl(O_2CAr)_4$ as precursors in the reaction with PPh_3 in an $MeCN–H_2O$ medium, the formation of diruthenium(II,III) and diruthenium(II) intermediate species, which may be structurally related to the intermediate compounds involved in the decarbonylation process occurring in the alcoholic media, has been observed. The final products of the reactions in $MeCN–H_2O$ medium are (μ-oxo)bis(μ-carboxylato)diruthenium(III) complexes, which we have reported[11] earlier. Herein we present the syntheses, properties, and molecular structures of the diruthenium(II,III) and diruthenium(II) complexes $Ru_2(OH_2)Cl(MeCN)(O_2CAr)_4(PPh_3)_2$ (**2**) and $Ru_2(OH_2)(MeCN)_2(O_2CAr)_4(PPh_3)_2$ (**3**). A preliminary communication reporting **2** (Ar = C_6H_4-*p*-OMe, C_6H_5) has been published.[12]

Experimental Section

Materials and Methods. Solvents and reagents were used generally as obtained from commercial sources. Acetone, benzene, chloroform, and dichloromethane used for electronic spectral measurement were purified by conventional methods. Dichloromethane used for electrochemical studies was finally distilled from calcium hydride before use. Tetrabutylammonium perchlorate (TBAP) was prepared by reacting tetrabutylammonium bromide with perchloric acid in water. The solid thus obtained was recrystallized twice before drying at 100 °C under vacuum.

Preparation of $Ru_2Cl(O_2CAr)_4$ (1). Complexes **1a** and **1b** (Ar = C_6H_5 (**1a**); Ar = C_6H_4-*p*-OMe (**1b**)) were prepared by following a literature procedure.[13] The complexes with Ar = C_6H_4-*p*-Me, C_6H_4-*p*-Cl, and C_6H_4-*p*-NO_2 were made in near-quantitative yield in a similar manner. To prepare these sparingly soluble compounds, 0.3 g of $Ru_2Cl(O_2CMe)_4$[9] was refluxed with $ArCO_2H$ (in a 1:6 molar ratio) in 40 mL of MeOH–H_2O (1:1 v/v) for ca. 4 h. Anal. Calcd for $Ru_2Cl(O_2CC_6H_4CH_3)_4$ (**1c**): C, 49.34; H, 3.60. Found: C, 49.13; H, 3.61. Calcd for $Ru_2Cl(O_2CC_6H_4Cl)_4$ (**1d**): C, 39.07; H, 1.86. Found: C, 38.84; H, 2.28. Calcd for $Ru_2Cl(O_2CC_6H_4NO_2)_4$ (**1e**): C, 37.24; H, 1.77; N, 6.21. Found: C, 36.23; H, 2.27; N, 6.04.

Preparation of $Ru_2(OH_2)Cl(MeCN)(O_2CAr)_4(PPh_3)_2$ (2) (Ar = C_6H_5 (2a), C_6H_4-*p*-OMe (2b), C_6H_4-*p*-Me (2c), C_6H_4-*p*-Cl (2d)). Complexes **2a**, **2c**, and **2d** were prepared by a general procedure in which **1** was reacted with PPh_3 (in a 1:2 mole ratio) in an $MeCN–H_2O$ mixture (ca. 5% H_2O) at 10 °C. A green solution was readily obtained. The solution was passed through a silica column in C_6H_6; a greenish yellow band was eluted out with a 4:1 C_6H_6–MeCN mixture. The column at this stage was blue in color, and further elution was continued till the eluate was colorless. The eluted greenish yellow solution was evaporated to dryness, redissolved in a 4:1 C_6H_6–MeCN mixture, and chromatographed again on the same column. On elution with the same mixture of solvents, the yellow solution coming out as the first fraction was collected and evaporated to dryness immediately. Yield for compounds **2a**, **2c**, and **2d** was in the range 8–10%.

To prepare **2b**, 0.5 g (0.6 mmol) of **1b** was stirred at 25 °C with 0.32 g (1.2 mmol) of PPh_3 for 30 min in 8 mL of MeCN. The resultant yellowish green solution was passed through a silica column in C_6H_6 and the first yellow band eluted out with a 4:1 C_6H_6–MeCN mixture and was collected and concentrated to ca. 5 mL in volume. The compound was obtained in the crystalline form from this solution after addition of diethyl ether followed by overnight cooling at −10 °C. The greenish yellow crystals were washed with a mixture of MeCN and diethyl ether and dried. Yield: 0.12 g (ca. 15%). C, H, N data [found (calcd)]: **2a**, 59.28 (60.66), 4.22 (4.21), 1.64 (1.07); **2b**, 58.14 (58.91), 4.41 (4.42), 0.77 (0.98); **2c**, 62.17 (61.68), 4.73 (4.63), 1.72 (1.03); **2d**, 55.20 (54.86), 3.55 (3.53), 1.27 (0.97).

Table I. Crystallographic Data for $Ru_2(OH_2)Cl(MeCN)(O_2CC_6H_4\text{-}p\text{-}OMe)_4(PPh_3)_2$ (**2b**) and $Ru_2(OH_2)(MeCN)_2(O_2CC_6H_4\text{-}p\text{-}NO_2)_4(PPh_3)_2\cdot 1.5CH_2Cl_2$ (**3e**)

compound	**2b**	**3e**
chem formula	$C_{70}H_{63}NO_{13}P_2ClRu_2$	$C_{68}H_{54}N_6O_{17}P_2Ru_2\cdot 1.5CH_2Cl_2$
fw	1425.8	1618.7
space group	$P\bar{1}$ (No. 2)	$P2_1/c$ (No. 14)
a, Å	13.538 (5)	23.472 (6)
b, Å	15.650 (4)	14.303 (3)
c, Å	18.287 (7)	23.256 (7)
α, deg	101.39 (3)	
β, deg	105.99 (4)	101.69 (2)
γ, deg	97.94 (8)	
V, Å^3	3574	7645
Z	2	4
T, °C	20	20
λ(Mo Kα), Å	0.7107	0.7107
ρ_{obsd}, g cm^{-3}	1.35	
ρ_{calcd}, g cm^{-3}	1.32	1.41
transm coeff,[a] %	80–100	91–100
$R(F_o)$[b]	0.1011	0.0849
$R_w(F_o)$[c]	0.1056	0.0971
g	0.002 881	0.008 000

[a] Correction applied. [b] $R = \sum||F_o| - |F_c||/\sum|F_o|$. [c] $R_w = [\sum w(|F_o| - |F_c|)^2/\sum w|F_o|^2]^{1/2}$; $w = k/[\sigma^2(F_o) + g(F_o)^2]$.

Under these reaction conditions the compound with Ar = C_6H_4-*p*-NO_2 could not be obtained.

Preparation of $Ru_2(OH_2)(MeCN)_2(O_2CAr)_4(PPh_3)_2$ (3) (Ar = C_6H_5 (3a), C_6H_4-*p*-OMe (3b), C_6H_4-*p*-Me (3c), C_6H_4-*p*-Cl (3d), C_6H_4-*p*-NO_2 (3e)). These compounds were obtained by following a general method of preparation. A 0.5-mmol quantity of complex **1** was reacted with 0.27 g (1 mmol) of PPh_3 in 20 mL of a $MeCN–H_2O$ mixture (4:1 v/v) under stirring for 12 h at 25 °C. The resulting yellow precipitate (**3e** is brown) was filtered off and washed first with an $MeCN–H_2O$ mixture and then washed with a small quantity of cold MeCN. The fine powder was then dried in vacuo over P_4O_{10}. Yields obtained for **3a** and **3c–e** were in the range 40–46%. Yield of **3b** was ca. 20% by using this synthetic procedure. Compound **3b** was isolated at a higher yield in a different way in which 0.42 g (0.5 mmol) of **1b** was reacted with a 0.27-g (1-mmol) quantity of PPh_3 in 15 mL of a $MeCN–H_2O$ (4:1 v/v) mixture for 20 min. The resulting dark brown solution was filtered and the filtrate was cooled at 5 °C for 48 h. The yellow crystals obtained were washed with $MeCN–H_2O$ and finally with cold MeCN and dried over P_4O_{10} under vacuum. Yield: 0.31 g (44%). Anal. Calcd for $Ru_2(OH_2)(MeCN)_2(O_2CC_6H_5)_4(PPh_3)_2$ (**3a**): C, 62.23; H, 4.42; N, 2.13. Found: C, 61.87; H, 4.52; N, 2.57. Anal. Calcd for $Ru_2(OH_2)(MeCN)_2(O_2CC_6H_4OCH_3)_4(PPh_3)_2$ (**3b**): C, 60.36; H, 4.61; N, 1.95. Found: C, 60.20; H, 4.65; N, 2.66. Anal. Calcd for $Ru_2(OH_2)(MeCN)_2(O_2CC_6H_4CH_3)_4(PPh_3)_2$ (**3c**): C, 63.19; H, 4.83; N, 2.05. Found: C, 61.92; H, 4.95; N, 2.04. Anal. Calcd for $Ru_2(OH_2)(MeCN)_2(O_2CC_6H_4Cl)_4(PPh_3)_2$ (**3d**): C, 56.31; H, 3.72; N, 1.93. Found: C, 55.57; H, 3.84; N, 2.40. Anal. Calcd for $Ru_2(OH_2)(MeCN)_2(O_2CC_6H_4NO_2)_4(PPh_3)_2$ (**3e**): C, 54.72; H, 3.62; N, 5.63. Found: C, 53.74; H, 3.76; N, 5.61.

Measurements. The elemental analyses were made with a Heraeus CHN-O-RAPID elemental analyzer. The ^1H NMR spectra were recorded with Bruker WH-270 and AC(AF) 200-MHz spectrometers. EPR data were obtained from a Varian E-line Century Series spectrometer working in the X-band of microwave radiation. Cyclic and differential-pulse voltammetric (CV and DPV) measurements were made using a three-electrode setup on a PAR Model 174A polarographic analyzer connected with a Houston Instruments Omnigraphic X-Y recorder. In the three-electrode configuration, a platinum button, a platinum wire, and a saturated calomel electrode were used as working, auxiliary, and reference electrodes, respectively. For all electrochemical measurements, the solvents contained 0.1 M Bu_4NClO_4 (TBAP) as a supporting electrolyte. The measurements were made at 25 °C, and the data are un-

---

(7) Norman, J. G., Jr.; Renzoni, G. E.; Case, D. A. *J. Am. Chem. Soc.* **1979**, *101*, 5256.

(8) Chakravarty, A. R.; Cotton, F. A.; Tocher, D. A. *J. Am. Chem. Soc.* **1984**, *106*, 6409. Chakravarty, A. R.; Cotton, F. A. *Inorg. Chem.* **1985**, *24*, 3584.

(9) Mitchell, R. W.; Wilkinson, G. *J. Chem. Soc., Dalton Trans.* **1973**, 846.

(10) Mandal, S. K.; Chakravarty, A. R. *Inorg. Chim. Acta* **1987**, *132*, 157.

(11) Das, B. K.; Chakravarty, A. R. *Inorg. Chem.* **1990**, *29*, 2078.

(12) Das, B. K.; Chakravarty, A. R. *Inorg. Chem.* **1990**, *29*, 1783.

(13) Das, B. K.; Chakravarty, A. R. *Polyhedron* **1988**, *7*, 685.

corrected for junction potentials. Ferrocene, (η-Cp)$_2$Fe, was used as a standard in order to verify the potentials observed against the saturated calomel electrode (SCE) and to obtain the *n* values of the redox reactions by peak current measurements. The Fe(II)/Fe(III) couple of ferrocene was observed at 0.51 V (vs SCE) under similar experimental conditions in CH_2Cl_2 containing 0.1 M TBAP at 25 °C. Magnetic measurement[14] was carried out in $CDCl_3$ with ca. 2% CH_2Cl_2 as a reference.

X-ray Crystallographic Procedures. The molecular structures of **2b** and **3e** were obtained by general procedures described[11] before. The crystal parameters and basic information pertaining to data collection and structure refinement[15-17] are summarized in Table I. Details of the crystal structure determination are presented as supplementary material. Crystals of **2b** were found to be thermally unstable. In **2b**, the aryl group atoms of a bridging carboxylato ligand, C22–C27, O23, and C28, were positionally disordered in a 1:1 fashion with C222–C272, O232, and C282. The disordered atoms were refined with a 0.5 occupancy factor. Besides these atoms, the Cl and MeCN atoms also showed relatively high thermal parameters. For **3e**, the CH_2Cl_2 molecules were in a highly disordered state.

Results

Synthesis and Reactions. When $Ru_2Cl(O_2CAr)_4$[18] (**1**) is reacted with PPh_3 in MeCN under stirring or refluxing condition, the product is a purple (μ-oxo)diruthenium(III) complex, $Ru_2O(O_2CAr)_4(PPh_3)_2$ (**4**). However, in the presence of a small amount of water (ca. 5%) the insoluble precursor complex reacts smoothly with PPh_3 with stirring in ca. 30 min. to give a green solution from which a mixed-valence diruthenium(II,III) compound can be isolated by column chromatographic separation. The other species present in the mixture is a blue complex, which is isolated as a perchlorate salt (**5**), $Ru_2O(MeCN)_4(O_2CAr)_2(PPh_3)_2(ClO_4)_2$ (eq 1). $Ru_2Cl(O_2CC_6H_4\text{-}p\text{-}OMe)_4$ reacts with PPh_3 in a similar

$$\mathrm{Ru_2Cl(O_2CAr)_4 + PPh_3 \xrightarrow[10\ ^{\circ}C]{MeCN-H_2O}} \\ \mathrm{[green\ solution] \xrightarrow[chromatography]{column} 2 + 5} \qquad (1)$$

manner without the addition of any extra H_2O to the commercial reagent grade MeCN containing ~0.3% H_2O. In all these cases, however, the product is a mixture of **2** and **3**. The highest purity (ca. 95%) that could be achieved was for **2b** (see electrochemical results). The diruthenium(II) compound **3** could not be isolated in the pure form by this method either. Both **2** and **3** are nonpolar and have similar solubility properties and are therefore not separable by conventional chromatographic techniques (no separation was observed in TLC also). Moreover, since **2** is unstable in solution, rapid elution is found to be necessary during column chromatographic separation.

The diruthenium(II) compounds (**3**) are prepared in analytically and spectroscopically pure form by carrying out the reaction in an MeCN–H_2O mixture (4:1 v/v) under stirring condition at 25 °C. After isolation of **3**, the blue filtrate is found to contain **5** and $ArCO_2H$. The reaction stoichiometry is given in eq 2. Under

$$\mathrm{[Ru_2Cl(O_2CAr)_4]_{\mathit{x}} + 2\mathit{x}PPh_3 \xrightarrow{MeCN-H_2O}} \\ \underset{\mathbf{3}}{(x/2)\mathrm{[Ru_2(OH_2)(MeCN)_2(O_2CAr)_4(PPh_3)_2]}} + \\ \underset{\mathbf{5}}{(x/2)\mathrm{[Ru_2O(MeCN)_4(O_2CAr)_2(PPh_3)_2]Cl_2}} + 2x\mathrm{ArCO_2H} \qquad (2)$$

the reaction conditions the formation of **4** is not observed. The formation of **3** and **5** in reaction 2 suggests the disproportionating nature of the reaction, which is mediated by the unstable mixed-valence species **2**.

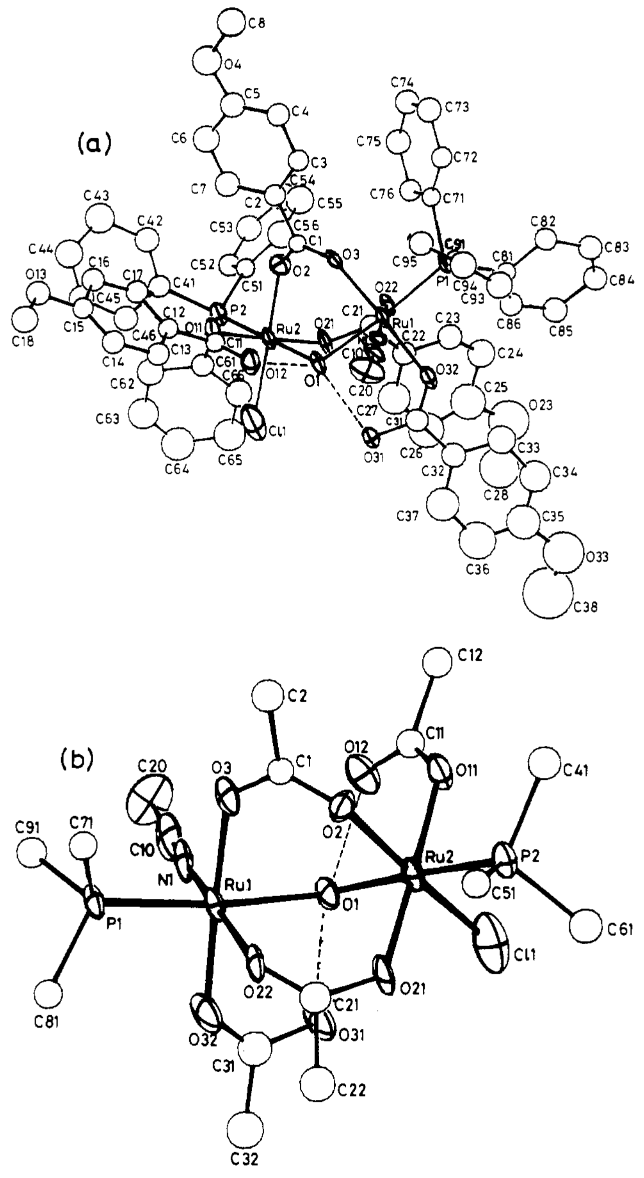

Figure 1. ORTEP views of the molecule (a) and the coordination sphere (b) of $Ru_2(OH_2)Cl(MeCN)(O_2CC_6H_4\text{-}p\text{-}OMe)_4(PPh_3)_2$ (**2b**).

Both **2** and **3** are unstable in the solution phase. Compound **2** is soluble in common organic solvents. While it converts rapidly in MeCN to the blue species **5**, in other solvents the purple compound **4** is the end product. In the latter case some other soluble, yet unidentified, compound forms along with **4**. Compound **3** is relatively more stable in the solution phase but on standing it also converts in a manner similar to that seen for **2**. Compound **2** decomposes even in the solid state at 25 °C, but it is moderately stable when kept at low temperature.

Molecular Structures. The structures of $Ru_2(OH_2)Cl(MeCN)(O_2CC_6H_4\text{-}p\text{-}OMe)_4(PPh_3)_2$ (**2b**) and $Ru_2(OH_2)(MeCN)_2(O_2CC_6H_4\text{-}p\text{-}NO_2)_4(PPh_3)_2\cdot 1.5CH_2Cl_2$ (**3e**) were obtained by single-crystal X-ray crystallographic studies. The ORTEP[17] diagrams of **2b** and **3e**, along with the atom numbering schemes, are shown in Figures 1 and 2, respectively. The selected atomic coordinates along with the isotropic thermal parameters are presented in Tables II and III, respectively, for **2b** and **3e**. Tables IV and V list the selected bond distances and angles for **2b** and **3e**, respectively. A comparison of the structural data on complexes[19-22] with an $\{M_2(\mu\text{-}OH_2)(\mu\text{-}O_2CR)_2{}^{2+}\}$ core is made

---

(14) Kozik, M.; Casan-Pastor, N.; Hammer, C. F.; Baker, L. C. W. *J. Am. Chem. Soc.* **1988**, *110*, 7697.

(15) (a) Sheldrick, G. M. In *Crystallographic Computing 3*; Sheldrick, G. M., Krüger, C., Goddard, R., Eds.; Clarendon Press: Oxford, England, 1985; pp 175–189. (b) Sheldrick, G. M. *A Program for Crystal Structure Determination*; Cambridge University Press: Cambridge, England, 1976.

(16) North, A. C. T.; Phillips, D. C.; Mathews, F. S. *Acta Crystallogr.* **1968**, *A24*, 351.

(17) Johnson, C. K. ORTEP. Report ORNL-3794; Oak Ridge National Laboratory: Oak Ridge, TN, 1971.

(18) Das, B. K.; Chakravarty, A. R. *Polyhedron* **1991**, *10*, 491.

(19) Turpeinen, U.; Hämäläinen, R. *Polyhedron* **1987**, *6*, 1603.

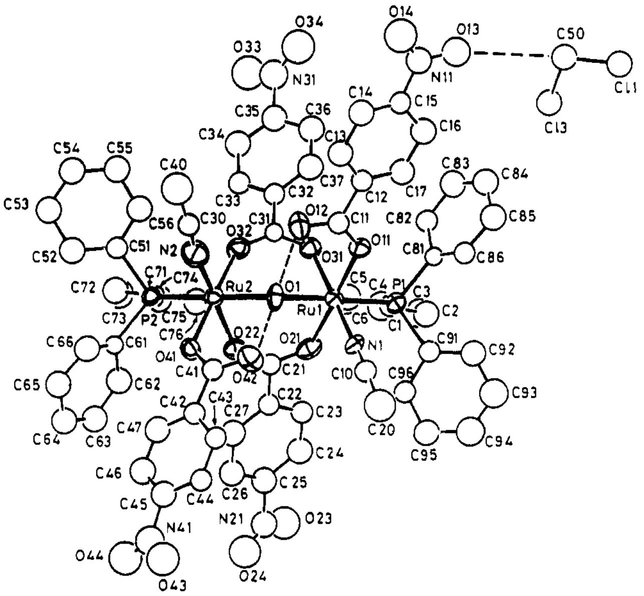

Figure 2. ORTEP view of $Ru_2(OH_2)(MeCN)_2(O_2CC_6H_4\text{-}p\text{-}NO_2)_4(PPh_3)_2$ (**3e**) along with the atom-labeling scheme. The CH_2Cl_2 molecule in contact with a *p*-nitro group is also shown.

Table II. Selected Atomic Coordinates and Equivalent Isotropic Thermal Parameters[a] ($\times 10^3$) with Esd's for **2b**

atom	*x/a*	*y/b*	*z/c*	U_{iso}, Å^2
Ru1	0.3887 (1)	0.1762 (1)	0.1558 (1)	38 (1)
Ru2	0.6650 (1)	0.2459 (1)	0.2620 (1)	41 (1)
P1	0.2284 (3)	0.2127 (3)	0.1270 (3)	43 (2)
P2	0.7932 (3)	0.3466 (3)	0.3616 (3)	47 (2)
Cl1	0.7452 (5)	0.1298 (5)	0.2830 (4)	122 (4)
O1	0.5430 (7)	0.1489 (7)	0.1732 (6)	46 (4)
O2	0.5931 (8)	0.3467 (7)	0.2323 (6)	47 (4)
O3	0.4434 (7)	0.2951 (7)	0.1304 (6)	47 (5)
O11	0.7369 (8)	0.2703 (8)	0.1796 (6)	60 (5)
O12	0.6325 (8)	0.1696 (8)	0.0738 (7)	67 (6)
O21	0.5894 (7)	0.2243 (8)	0.3425 (7)	60 (5)
O22	0.4224 (8)	0.2270 (7)	0.2763 (6)	50 (5)
O31	0.4877 (9)	0.0042 (9)	0.1968 (10)	91 (8)
O32	0.3401 (8)	0.0557 (7)	0.1828 (7)	57 (6)
N1	0.3634 (9)	0.1128 (8)	0.0450 (9)	44 (6)
C10	0.3558 (14)	0.0770 (12)	−0.0160 (13)	63 (10)
C20	0.3467 (22)	0.0328 (16)	−0.0967 (12)	111 (14)
C1	0.5250 (11)	0.3539 (10)	0.1722 (8)	38 (4)
C2	0.5337 (14)	0.4410 (12)	0.1462 (10)	56 (5)
C11	0.7070 (12)	0.2318 (10)	0.1066 (9)	43 (4)
C12	0.7724 (13)	0.2717 (11)	0.0605 (10)	50 (4)
C21	0.4927 (13)	0.2193 (11)	0.3353 (10)	49 (4)
C22	0.4573 (31)	0.1682 (28)	0.3920 (23)	67 (11)
C222	0.4667 (26)	0.2414 (23)	0.4144 (20)	47 (8)
C31	0.3936 (14)	0.0012 (12)	0.2002 (10)	60 (5)
C32	0.3469 (17)	−0.0739 (14)	0.2302 (12)	75 (6)
C41	0.8811 (14)	0.4202 (12)	0.3277 (10)	55 (5)
C51	0.7461 (12)	0.4222 (10)	0.4294 (9)	45 (4)
C61	0.8770 (15)	0.2933 (12)	0.4318 (11)	63 (5)
C71	0.2327 (11)	0.3341 (10)	0.1509 (9)	39 (4)
C81	0.1329 (12)	0.1726 (10)	0.1754 (9)	43 (4)
C91	0.1619 (13)	0.1810 (11)	0.0212 (10)	50 (4)
H1	0.5128	0.0825	0.1579	80
H2	0.5715	0.1376	0.1379	80

[a] Atoms Ru1 to C20, which were refined anistropically, have been given an equivalent isotropic displacement parameter defined as U_{iso}(eq) = $[\sum_i\sum_j U_{ij}a^*_i\cdot a^*_j\cdot a_i\cdot a_j]/3$. For the isotropic atoms (C1 to H2) U_{11} values are given. For hydrogen atoms the U_{11} value is arbitrarily chosen.

in Table VI.

Table III. Selected Atomic Coordinates and Equivalent Isotropic Thermal Parameters[a] ($\times 10^3$) with Esd's for **3e**

atom	*x/a*	*y/b*	*z/c*	U_{iso}, Å^2
Ru1	0.1979 (1)	0.4922 (1)	0.3088 (1)	32 (1)
Ru2	0.3029 (1)	0.5001 (1)	0.2091 (1)	33 (1)
P1	0.1419 (1)	0.4057 (2)	0.3564 (1)	34 (1)
P2	0.3577 (1)	0.4198 (2)	0.1567 (1)	35 (1)
O1	0.2513 (3)	0.5743 (5)	0.2614 (4)	40 (3)
N1	0.1342 (4)	0.5830 (7)	0.2797 (4)	35 (3)
N2	0.3661 (4)	0.5890 (7)	0.2406 (4)	65 (4)
O11	0.2285 (3)	0.5728 (6)	0.3840 (4)	43 (3)
O12	0.3030 (4)	0.6440 (7)	0.3548 (4)	62 (4)
O21	0.1683 (3)	0.4095 (6)	0.2353 (4)	46 (3)
O22	0.2310 (4)	0.4187 (7)	0.1731 (4)	53 (3)
O31	0.2713 (3)	0.4100 (6)	0.3414 (4)	44 (3)
O32	0.3336 (4)	0.4115 (6)	0.2801 (4)	47 (3)
O41	0.2702 (4)	0.5834 (6)	0.1359 (3)	45 (3)
O42	0.2083 (5)	0.6742 (7)	0.1755 (4)	67 (4)
C10	0.0976 (6)	0.6308 (10)	0.2612 (6)	52 (4)
C20	0.0498 (8)	0.6963 (14)	0.2367 (9)	97 (6)
C30	0.4003 (6)	0.6409 (10)	0.2635 (6)	49 (3)
C40	0.4467 (9)	0.7070 (15)	0.2891 (10)	107 (7)
C11	0.2736 (5)	0.6224 (9)	0.3922 (6)	45 (3)
C12	0.2981 (5)	0.6517 (9)	0.4564 (6)	42 (3)
C21	0.1857 (5)	0.3919 (9)	0.1872 (5)	42 (3)
C22	0.1455 (5)	0.3326 (9)	0.1444 (6)	42 (3)
C31	0.3175 (5)	0.3889 (8)	0.3269 (5)	37 (3)
C32	0.3589 (5)	0.3299 (9)	0.3682 (6)	42 (3)
C41	0.2285 (5)	0.6400 (9)	0.1321 (6)	44 (3)
C42	0.1996 (6)	0.6699 (9)	0.0716 (6)	44 (3)
C51	0.4368 (5)	0.4396 (8)	0.1787 (5)	40 (3)
C61	0.3387 (5)	0.4369 (8)	0.0763 (5)	34 (3)
C71	0.3554 (5)	0.2919 (8)	0.1607 (5)	41 (3)
C81	0.1574 (5)	0.4174 (8)	0.4365 (5)	35 (3)
C91	0.0627 (6)	0.4229 (9)	0.3328 (6)	45 (3)
C1	0.1447 (5)	0.2787 (8)	0.3485 (6)	40 (3)

[a] Atoms Ru1 to C40, which were refined anisotropically, have been given an equivalent isotropic displacement parameter defined as U_{iso}(eq) = $[\sum_i\sum_j U_{ij}a^*_i\cdot a^*_i\cdot a_i\cdot a_j]/3$. For the isotropic atoms (C11 to C1) U_{11} values are given.

Both of the molecules, **2b** and **3e**, consist of a diruthenium unit held by an aqua bridge and two bridging carboxylato ligands. The bridging ligands occupy a face of the octahedron leaving the three other facial coordination sites on each metal center to be occupied by other ligands. An interesting feature in **2** and **3** is that the facial sites are occupied by three ligands of varying π-acidity. In **2**, the facial ligands on one metal are PPh_3, Cl, and η^1-O_2CAr while the other has PPh_3, MeCN, and η^1-O_2CAr. In **3**, the facial ligands on the metal centers are PPh_3, MeCN, and η^1-O_2CAr.

The aqua bridge in **2** and **3** is stabilized by strong hydrogen-bonding interactions with two η^1-bonded O_2CAr ligands bonded to the metal centers. The O(aquo)···O(carboxylato) contact distances are nearly 2.5 Å. A similar type of hydrogen bonding involving the $\{M_2(\mu\text{-}OH_2)(\mu\text{-}O_2CR)_2(\eta^1\text{-}O_2CR)_2\}$ core is known[19-22] in other complexes (Table VI). The trans arrangement of PPh_3 in **2** and **3** is due to the presence of two intramolecular hydrogen bonds. The P–Ru–OH_2 geometries are essentially linear. In the (μ-oxo)diruthenium(III) complexes[11] **4** and **5**, the P–Ru–O(oxo) angles are nearly 90°. This suggests that during the oxidation of **2** and **3** to form **4** and **5**, a core rearrangement, assisted by the removal of the hydrogen-bonding interactions, takes place, bringing the PPh_3 ligands cis to the μ-oxo ligand in **4** and **5**.

The metal centers in the asymmetric molecule **2b** are clearly distinguishable. In the coordination spheres the Ru1–O distances are longer than the corresponding Ru2–O distances. This suggests that the oxidation states for Ru1 and Ru2 are +2 and +3, respectively. This result is commensurate with our expectation since the chloride ligand is bonded to Ru2. Compound **2** thus exem-

---

(20) Turpeinen, U.; Ahlgrén, M.; Hämäläinen, R. *Acta Crystallogr.* **1982**, *B38*, 1580.

(21) Turpeinen, U.; Ahlgrén, M.; Hämäläinen, R. *Finn. Chem. Lett.* **1977**, 146.

(22) (a) Albers, M. O.; Liles, D. C.; Singleton, E.; Yates, J. E. *J. Organomet. Chem.* **1984**, *272*, C62. (b) Albers, M. O.; Liles, D. C.; Singleton, E.; Stead, J. E. *Acta Crystallogr.* **1986**, *C42*, 46. (c) Albers, M. O.; Liles, D. C.; Singleton, E.; Stead, J. E. *Acta Crystallogr.* **1986**, *C42*, 1299.

Table IV. Selected Bond Distances (Å) and Bond Angles (deg) for **2b** with Esd's in Parentheses

Distances			
Ru(1)–Ru(2)	3.604 (1)	Ru(2)–O(1)	2.127 (8)
Ru(1)–O(1)	2.141 (10)	Ru(2)–P(2)	2.277 (4)
Ru(1)–P(1)	2.268 (4)	Ru(2)–Cl(1)	2.283 (8)
Ru(1)–N(1)	1.984 (15)	Ru(2)–O(2)	2.050 (11)
Ru(1)–O(3)	2.093 (11)	Ru(2)–O(11)	2.072 (13)
Ru(1)–O(22)	2.086 (11)	Ru(2)–O(21)	2.064 (13)
Ru(1)–O(32)	2.106 (13)	N(1)–C(10)	1.114 (27)
C(10)–C(20)	1.465 (32)	O(2)–C(1)	1.262 (17)
O(3)–C(1)	1.276 (15)	O(11)–C(11)	1.275 (18)
O(12)–C(11)	1.220 (17)	O(21)–C(21)	1.269 (20)
O(22)–C(21)	1.266 (19)	O(31)–C(31)	1.288 (24)
O(32)–C(31)	1.227 (23)	O(1)–H(1)	1.105
O(31)–H(1)	1.577	O(1)–H(2)	0.841
O(12)–H(2)	1.720	O(1)–O(12)	2.493 (18)
O(1)–O(31)	2.443 (19)		
Angles			
Ru(1)–O(1)–Ru(2)	115.2 (5)	O(1)–Ru(1)–P(1)	173.6 (4)
O(1)–Ru(1)–N(1)	84.4 (5)	P(1)–Ru(1)–N(1)	92.1 (4)
O(1)–Ru(1)–O(3)	88.0 (4)	P(1)–Ru(1)–O(3)	86.7 (3)
O(1)–Ru(1)–O(22)	90.8 (4)	P(1)–Ru(1)–O(22)	93.3 (3)
O(1)–Ru(1)–O(32)	89.7 (4)	P(1)–Ru(1)–O(32)	95.7 (3)
N(1)–Ru(1)–O(3)	89.2 (5)	N(1)–Ru(1)–O(22)	171.9 (5)
N(1)–Ru(1)–O(32)	90.8 (5)	O(3)–Ru(1)–O(22)	97.0 (4)
O(3)–Ru(1)–O(32)	177.6 (4)	O(22)–Ru(1)–O(32)	82.7 (4)
O(1)–Ru(2)–P(2)	177.2 (4)	O(1)–Ru(2)–Cl(1)	85.9 (3)
O(1)–Ru(2)–O(11)	90.4 (4)	O(1)–Ru(2)–O(2)	91.2 (4)
O(1)–Ru(2)–O(21)	89.2 (4)	P(2)–Ru(2)–Cl(1)	93.0 (2)
P(2)–Ru(2)–O(2)	90.1 (3)	P(2)–Ru(2)–O(11)	92.3 (3)
P(2)–Ru(2)–O(21)	88.2 (3)	Cl(1)–Ru(2)–O(2)	174.6 (4)
Cl(1)–Ru(2)–O(11)	93.0 (4)	Cl(1)–Ru(2)–O(21)	89.0 (4)
O(2)–Ru(2)–O(11)	82.4 (5)	O(2)–Ru(2)–O(21)	95.6 (5)
O(11)–Ru(2)–O(21)	177.9 (5)	O(2)–C(1)–O(3)	125.8 (15)
O(11)–C(11)–O(12)	125.0 (17)	O(21)–C(21)–O(22)	126.5 (18)
O(31)–C(31)–O(32)	124.5 (19)	Ru(1)–N(1)–C(10)	175.5 (14)
N(1)–C(10)–C(20)	178.1 (21)	O(1)–H(1)–O(31)	140.1
O(1)–H(2)–O(12)	151.7	H(1)–O(1)–H(2)	85.5

Table V. Selected Bond Distances (Å) and Bond Angles (deg) for **3e** with Esd's in Parentheses

Distances			
Ru(1)–Ru(2)	3.712 (1)	Ru(2)–P(2)	2.257 (4)
Ru(1)–P(1)	2.254 (3)	Ru(2)–O(1)	2.162 (9)
Ru(1)–O(1)	2.173 (9)	Ru(2)–N(2)	1.978 (10)
Ru(1)–N(1)	1.994 (9)	Ru(2)–O(22)	2.083 (9)
Ru(1)–O(11)	2.097 (8)	Ru(2)–O(32)	2.091 (8)
Ru(1)–O(21)	2.078 (8)	Ru(2)–O(41)	2.091 (8)
Ru(1)–O(31)	2.095 (8)	N(1)–C(10)	1.112 (16)
N(2)–C(30)	1.143 (16)	C(10)–C(20)	1.486 (23)
C(30)–C(40)	1.474 (24)	O(11)–C(11)	1.258 (15)
O(12)–C(11)	1.253 (18)	O(21)–C(21)	1.293 (17)
O(22)–C(21)	1.234 (16)	O(31)–C(31)	1.237 (15)
O(32)–C(31)	1.265 (16)	O(41)–C(41)	1.260 (15)
O(42)–C(41)	1.294 (14)	O(1)–O(12)	2.473 (12)
O(1)–O(42)	2.497 (12)	O(13)–C(50)	3.368 (21)
Angles			
Ru(1)–O(1)–Ru(2)	117.8 (4)	O(1)–Ru(1)–P(1)	179.0 (2)
O(1)–Ru(1)–O(11)	89.5 (3)	O(1)–Ru(1)–O(21)	91.3 (3)
O(1)–Ru(1)–O(31)	88.4 (3)	O(1)–Ru(1)–N(1)	86.8 (4)
O(11)–Ru(1)–O(21)	178.7 (3)	O(11)–Ru(1)–O(31)	83.7 (3)
O(11)–Ru(1)–P(1)	91.5 (3)	O(11)–Ru(1)–N(1)	91.8 (3)
O(21)–Ru(1)–O(31)	95.3 (3)	O(21)–Ru(1)–P(1)	87.7 (3)
O(21)–Ru(1)–N(1)	173.4 (4)	N(1)–Ru(1)–P(1)	93.0 (3)
O(1)–Ru(2)–P(2)	178.3 (2)	O(22)–Ru(2)–P(2)	90.1 (3)
O(1)–Ru(2)–O(22)	89.9 (3)	O(22)–Ru(2)–O(32)	95.7 (3)
O(1)–Ru(2)–O(32)	89.8 (3)	O(22)–Ru(2)–O(41)	81.8 (3)
O(1)–Ru(2)–O(41)	91.3 (3)	O(22)–Ru(2)–N(2)	174.1 (4)
O(1)–Ru(2)–N(2)	86.6 (4)	O(32)–Ru(2)–P(2)	88.5 (3)
O(32)–Ru(2)–O(41)	177.3 (3)	O(32)–Ru(2)–N(2)	89.1 (4)
O(41)–Ru(2)–P(2)	90.4 (3)	O(41)–Ru(2)–N(2)	93.5 (4)
Ru(1)–N(1)–C(10)	176.5 (10)	Ru(2)–N(2)–C(30)	173.3 (12)
N(1)–C(10)–C(20)	178.7 (16)	N(2)–C(30)–C(40)	175.4 (17)
O(11)–C(11)–O(12)	126.8 (12)	O(21)–C(21)–O(22)	127.7 (11)
O(31)–C(31)–O(32)	127.1 (11)	O(41)–C(41)–O(42)	126.1 (11)
Cl(1)–C(50)–Cl(3)	107.0 (8)		

Table VI. Structural Comparison for Complexes with an $\{M_2(\mu\text{-}OH_2)(\mu\text{-}O_2CR)_2{}^{n+}\}$ Core

compound	M–M, Å	M–O–M, deg	M–OH$_2$, Å	ref
$Co_2(OH_2)(O_2CCCl_3)_4(tmen)_2$[a]	3.696	116.1	2.180	19
$Co_2(OH_2)(O_2CCH_3)_4(tmen)_2$	3.596	115.1	2.137	20
$Ni_2(OH_2)(O_2CCH_3)_4(tmen)_2$	3.563	117.2	2.088	21
$Ru_2(OH_2)(O_2CCF_3)_4(cod)_2$[b]	3.733	119.2	2.164	22a
$Ru_2(OH_2)(O_2CCF_3)_4(PMe_2Ph)_4$	3.881	120.7	2.233	22b
$Ru_2(OH_2)(O_2CCCl_3)_4(nor)_2$[c]	3.675	117.3	2.152	22c
$Ru_2(OH_2)(MeCN)_2$-$(O_2CC_6H_4\text{-}p\text{-}NO_2)_4(PPh_3)_2$	3.712	117.8	2.173 2.162	this work
$Ru_2(OH_2)Cl(MeCN)$-$(O_2CC_6H_4\text{-}p\text{-}OMe)_4(PPh_3)_2$	3.604	115.2	2.141 2.127	this work

[a] tmen, tetramethylethylenediamine. [b] cod, cyclooctadiene. [c] nor, norbornadiene.

Table VII. Near-IR and EPR[a,b] Spectra Data for $Ru_2(OH_2)Cl(MeCN)(O_2CAr)_4(PPh_3)_2$

	IT band		*g* values	
compound	solvent	λ_{max}, nm	$g_\parallel$	$g_\perp$
2a (Ar = C_6H_5)	$CHCl_3$	920	1.70	2.35
2b (Ar = C_6H_4-*p*-OMe)	$CHCl_3$	960	1.70	2.35
	CH_2Cl_2	947		
	Me_2CO	924		
	C_6H_6	915		
2c (Ar = C_6H_4-*p*-Me)	$CHCl_3$	935	1.70	2.29
2d (Ar = C_6H_4-*p*-Cl)	$CHCl_3$	900	1.69	2.28

[a] Polycrystalline state; DPPH as standard, 25 °C. [b] **2b**, rhombic spectrum in benzene glass at −140 °C; g_1, 2.35; g_2, 2.25; g_3, 1.70.

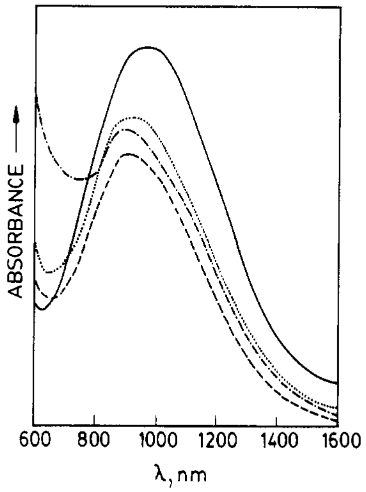

Figure 3. The intervalence transfer (IT) bands in **2** in $CHCl_3$: (– –) **2a**; (—) **2b**; (···) **2c**; (–·–) **2d**.

plifies an asymmetric, trapped mixed-valence system with localized oxidation states.

Spectral Properties. Electronic spectra of the mixed-valence compounds **2** exhibit a broad and weak absorption band in the range 900–960 nm in $CHCl_3$ as shown in Figure 3. The relevant data are presented in Table VII. The band, which is absent in the electronic spectra of **3**, **4**, and **5**, is assignable to an intervalence (IT) transition. This band has a width at half-intensity of 4820 cm^{-1} against the expected[23,24] value of 4900 cm^{-1}. Further, the band positions depend upon the polarity and nature of solvent (Table VII). Molecule **2b** is thus a trapped-valence species of class II type in the Robin and Day classification of mixed-valence systems.[25] The molar extinction coefficient of **2b** is 575 M^{-1} cm^{-1} in $CHCl_3$. For other complexes ε was not determined because of the presence of varying amount of **3** as an impurity. The magnitude of interaction between the metal centers, H_{AB}, cal-

---

(23) Creutz, C. *Prog. Inorg. Chem.* **1983**, *30*, 1.

(24) Hush, N. S. *Prog. Inorg. Chem.* **1967**, *8*, 391.

(25) Robin, M. B.; Day, P. *Adv. Inorg. Chem. Radiochem.* **1967**, *10*, 247.

Table VIII. ^1H NMR Data[a,b] on $Ru_2(OH_2)(MeCN)_2(O_2CAr)_4(PPh_3)_2$ (3)

compound	MeCN	X = Me (C_6H_4-*p*-X)	Ar	PPh_3	μ-H_2O
3a (Ar = C_6H_5)	2.24 s (6 H)		6.67–7.17 m (14 H) 7.54 d (6 H, *J* = 7.1)	7.20–7.55 m (18 H) 7.82 t[c] (12 H, J^d = 8.4)	16.96 s (2 H)
3b (Ar = C_6H_4-*p*-OMe)	2.23 s (6 H)	3.62 s (6 H) 3.76 s (6 H)	6.20 d (4 H, *J* = 8.5) 6.63 d (4 H, *J* = 8.5) 6.74 d (4 H, *J* = 8.5) 7.48 d (4 H, *J* = 8.2)	7.21–7.30 m (18 H) 7.81 t[c] (12 H, *J* = 8.5)	16.94 s (2 H)
3c (Ar = C_6H_4-*p*-Me)	2.21 s (6 H)	2.11 s (6 H) 2.28 s (6 H)	6.50 d (4 H, *J* = 8.0) 6.67 d (4 H, *J* = 8.0) 6.93 d (4 H, *J* = 7.9) 7.41 d (4 H, *J* = 8.0)	7.21–7.30 m (18 H) 7.81 t[c] (12 H, *J* = 8.5)	16.98 s (2 H)
3d (Ar = C_6H_4-*p*-Cl)	2.26 s (6 H)		6.64 m[e] (8 H, J_1 = 8.7, J_2 = 3.6, J_3 = 8.7) 7.10 d (4 H, *J* = 8.5) 7.42 d (4 H, *J* = 8.5)	7.22–7.36 m (18 H) 7.74 t[c] (12 H, *J* = 8.5)	16.73 s (2 H)
3e (Ar = C_6H_4-*p*-NO_2)	2.35 s (6 H)		6.79 d (4 H, *J* = 8.6) 7.56 d (4 H, *J* = 8.5) 7.63 d (4 H, *J* = 8.4) 8.01 d (4 H, *J* = 8.5)	7.22–7.51 m (18 H) 7.73 t[c] (12 H, *J* = 8.6)	16.53 s (2 H)

[a] In $CDCl_3$ with TMS as reference. [b] Chemical shifts, ppm. [c] Key: s, singlet; d, doublet; t, triplet; m, multiplet. [c] Apparent triplet. [d] *J*, Hz. [e] AB pattern.

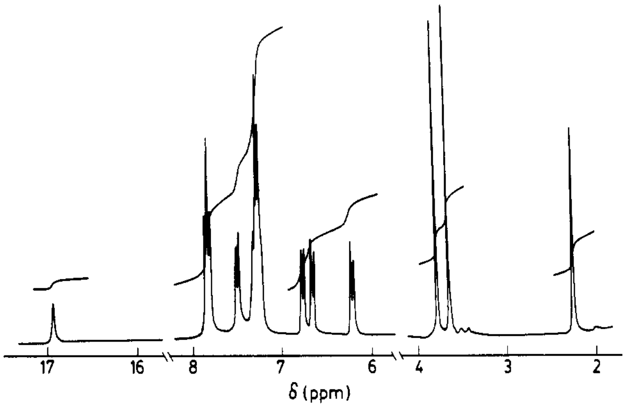

Figure 4. ^1H NMR spectrum of $Ru_2(OH_2)(MeCN)_2(O_2CC_6H_4$-*p*-$OMe)_4(PPh_3)_2$ (**3b**) in $CDCl_3$.

culated according to the Hush formula[23,24] for **2b** was found to be ca. 965 cm^{-1}.

Compound **2** is paramagnetic[12,26] and exhibits characteristic EPR spectra of a t_{2g}^5 Ru(III) species in an axial field. In benzene glass at −140 °C, **2b** shows a rhombic spectrum which is expected from the coordination geometry of the Ru(III) center (Figure 1). Relevant EPR data on **2** are presented in Table VII. As the g_1 and g_2 values are not very different,[12] in the polycrystalline state only an axial spectrum is observed. Since complex **2** was found to be mixed with **3** as an impurity, the magnetic susceptibility measurements were carried out only for **2b**, which showed a μ_{eff} value of 2.32 μ_B at 25 °C.

The diamagnetic diruthenium(II) compounds (**3**) show interesting ^1H NMR spectra. The data are presented in Table VIII, and a representative spectrum is shown in Figure 4. The μ-aquo resonance appearing as a singlet in the range 16.53–16.98 ppm indicates the presence of strong hydrogen-bonding interactions involving the μ-aquo ligand that deshield the protons. The para-substituted C_6H_4 groups for η^1-O_2CAr and $\eta^1{:}\eta^1{:}\mu_2$-O_2CAr ligands appear as two pairs of equal intensity doublets, the only exception being **3d** where an AB pattern is seen in place of a pair of doublets.

Electrochemistry. The electron-transfer properties of **2** and **3** were studied by cyclic and differential-pulse voltammetric techniques using a platinum working electrode in CH_2Cl_2 containing 0.1 M TBAP as a supporting electrolyte. The electrochemical data on **2** and **3** are given in Tables IX and X, respectively.

Table IX. Cyclic Voltammetric (CV)[a] and Differential-Pulse Voltammetric (DPV)[b] Data for $Ru^{II}Ru^{III}(OH_2)Cl(MeCN)$-$(O_2CAr)_4(PPh_3)_2$ (**2**) in CH_2Cl_2 Containing 0.1 M TBAP

	$Ru^{II}Ru^{III}/Ru_2^{II}$		$Ru^{II}Ru^{III}/Ru_2^{III}$	
compound	CV data $E_{1/2}$, V (ΔE_p, mV)	DPV data E_{fs}, V (δ, mV)	CV data $E_{1/2}$, V (ΔE_p, mV)	DPV data E_{fs}, V (δ, mV)
2a (Ar = C_6H_5)	−0.39 (60)	−0.39 (100)	+0.66 (60)	+0.63 (100)
2b (Ar = C_6H_4-*p*-OMe)	−0.44 (100)	−0.43 (110)	+0.58 (80)	+0.57 (110)
2c (Ar = C_6H_4-*p*-Me)	−0.43 (100)	−0.42 (110)	+0.63 (80)	+0.62 (120)
2d (Ar = C_6H_4-*p*-Cl)	−0.32 (70)	−0.31 (100)	+0.75 (60)	+0.73 (90)

[a] Scan rate, 20 mV s^{-1}; $E_{1/2} = (E_{pa} + E_{pc})/2$; $\Delta E_p = E_{pa} - E_{pc}$. [b] Scan rate, 2 mV s^{-1}; modulation amplitude, 50 mV (pp); drop time, 0.5 s; E_{fs}, forward scan peak potential; δ, peak width at half-height.

Table X. Cyclic Voltammetric Data for $Ru^{II}_2(OH_2)(MeCN)_2(O_2CAr)_4(PPh_3)_2$ (**3**) at 20 mV s^{-1} in CH_2Cl_2 Containing 0.1 M TBAP

	$E_{1/2}$, V vs SCE (ΔE_p, mV)	
compound	$Ru^{II}_2/Ru^{II}Ru^{III}$	$Ru^{II}Ru^{III}/Ru^{III}_2$
3a (Ar = C_6H_5)	0.28 (90)	0.98 (100)
3b (Ar = C_6H_5-*p*-OMe)	0.21 (80)	0.88 (80)
3c (Ar = C_6H_5-*p*-Me)	0.23 (90)	0.92 (90)
3d (Ar = C_6H_5-*p*-Cl)	0.38 (80)	1.05 (80)
3e (Ar = C_6H_5-*p*-NO_2)	0.52 (80)	1.11 (130)

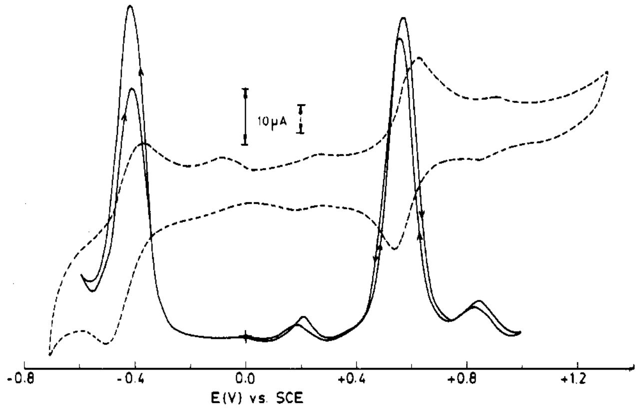

Figure 5. Cyclic and differential pulse voltammograms of $Ru_2(OH_2)$-$Cl(MeCN)(O_2CC_6H_4$-*p*-$OMe)_4(PPh_3)_2$ (**2b**) in CH_2Cl_2 containing 0.1 M TBAP at scan rates of 20 and 2 mV s^{-1}, respectively.

---

(26) The ^1H NMR spectra of **2** are complicated. For **2b** the μ-OH_2 ligand shows two signals at δ 18.0 and δ 10.2, which disappear upon addition of D_2O. The presence of four chemically nonequivalent carboxylato ligands along with the CH_3CN ligand is observed in the spectrum. Some of the para-substituted phenyl ring protons of the carboxylato ligands appear in the range δ 4–6.

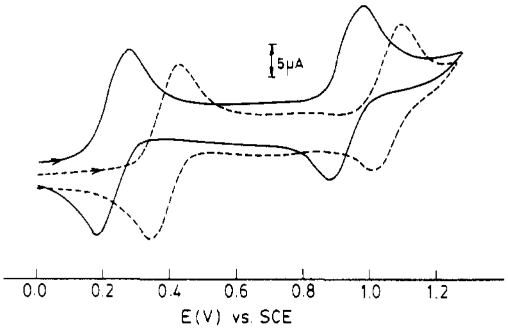

Figure 6. Cyclic voltammograms of $\mathrm{Ru_2(OH_2)(MeCN)_2(O_2CAr)_4(PPh_3)_2}$ with Ar = $\mathrm{C_6H_4}$-*p*-Me (**3c**, —) and Ar = $\mathrm{C_6H_4}$-*p*-Cl (**3d**, --) in $\mathrm{CH_2Cl_2}$ containing 0.1 M TBAP at a scan rate of 20 mV $\mathrm{s^{-1}}$.

Compound **2** undergoes two one-electron redox processes in the potential ranges −0.3 to −0.5 V and +0.5 to +0.8 vs SCE. The controlled-potential electrolysis showed that the response at the negative potential is due to a one-electron reduction while the response at the positive potential is due to a one-electron oxidation. The couples involved are given in eq 3. The one-electron stoichiometry of the redox couples was obtained from the peak current measurements using ferrocene as a standard. The differential-pulse voltammetric (DPV) technique has been used to determine the purity of **2** in a mixture of **2** and **3**. It was found that **2b** has only a trace of **3b**. The observed differential pulse and cyclic voltammograms are shown in Figure 5. Compounds **2a**, **2c** and **2d** were found to be pure to the extent of 60–70%. The remaining compound in the mixture is **3** in all the cases. The ΔE_p values in **2** indicate a nearly reversible nature of the reduction and oxidation processes. The i_{pa}/i_{pc} values for the reduction process, which are substantially less than 1.0, suggest that the reduced species undergoes decomposition under the experimental time scale. Thus an ECE mechanism[27] is likely to be operative in the process. The i_{pa}/i_{pc} ratio is ~1.0 for the oxidation process at various scan rates.

$$\underset{\mathbf{2'^+}}{\{\mathrm{Ru^{III}}_2(\mu\text{-OH}_2)(\mu\text{-O}_2\mathrm{CAr})_2{}^{4+}\}} \underset{-e}{\overset{+e}{\rightleftharpoons}} \underset{\mathbf{2'}}{\{\mathrm{Ru^{II}Ru^{III}}(\mu\text{-OH}_2)(\mu\text{-O}_2\mathrm{CAr})_2{}^{3+}\}}$$

$$\mathbf{2'} \underset{-e}{\overset{+e}{\rightleftharpoons}} \underset{\mathbf{2'^-}}{\{\mathrm{Ru^{II}}_2(\mu\text{-OH}_2)(\mu\text{-O}_2\mathrm{CAr})_2{}^{2+}\}} \quad (3)$$

The diruthenium(II) compound **3** undergoes two one-electron oxidation processes in the potential ranges +0.21 to +0.52 V and +0.88 to +1.11 V vs SCE. The electron-transfer processes are quasireversible in nature. The redox couples involved are given in eq 4, and representative voltammograms are shown in Figure 6. The $\{\mathrm{Ru_2}(\mu\text{-OH}_2)^{6+}\}$ cores of $\mathbf{3'^{2+}}$ and $\mathbf{2'^+}$ seem to be stable only on the CV time scale. The stability of the species follows the order $\mathbf{2'^+} > \mathbf{3'^{2+}}$. Such a core is expected to undergo a facile $\{\mathrm{Ru_2}(\mu\text{-OH}_2)^{6+}\}$ to $\{\mathrm{Ru_2}(\mu\text{-O})^{4+}\}$ core conversion, which is likely to be assisted by the presence of two η^1-$\mathrm{O_2CAr}$ facial ligands (eqs 2 and 5).

$$\underset{\mathbf{3'^{2+}}}{\{\mathrm{Ru^{III}}_2(\mu\text{-OH}_2)(\mu\text{-O}_2\mathrm{CAr})_2{}^{4+}\}} \underset{-e}{\overset{+e}{\rightleftharpoons}} \underset{\mathbf{3'^+}}{\{\mathrm{Ru^{II}Ru^{III}}(\mu\text{-OH}_2)(\mu\text{-O}_2\mathrm{CAr})_2{}^{3+}\}} \underset{-e}{\overset{+e}{\rightleftharpoons}} \underset{\mathbf{3'}}{\{\mathrm{Ru^{II}}_2(\mu\text{-OH}_2)(\mu\text{-O}_2\mathrm{CAr})_2{}^{2+}\}} \quad (4)$$

$$\{\mathrm{Ru^{III}}_2(\mu\text{-OH}_2)(\mu\text{-O}_2\mathrm{CAr})_2(\eta^1\text{-O}_2\mathrm{CAr})_2{}^{2+}\} \xrightarrow{\mathrm{MeCN}} \{\mathrm{Ru^{III}}_2(\mu\text{-O})(\mu\text{-O}_2\mathrm{CAr})_2(\mathrm{MeCN})_2{}^{2+}\} + 2\mathrm{ArCO_2H} \quad (5)$$

Scheme I. Reaction Pathways Involving the (μ-Aquo/μ-oxo)diruthenium Complexes[a]

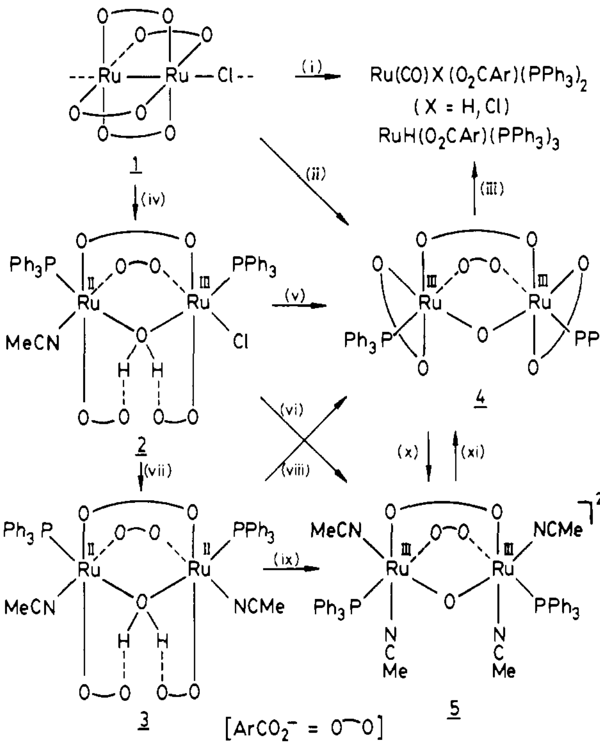

[a] Key: (i) $\mathrm{R'CH_2OH}$, excess $\mathrm{PPh_3}$, reflux; (ii) MeCN, $\mathrm{PPh_3}$, reflux; (iii) MeOH, excess $\mathrm{PPh_3}$, reflux; (iv) MeCN–$\mathrm{H_2O}$, $\mathrm{PPh_3}$, 10 °C; (v) $\mathrm{CHCl_3}$ at room temperature or MeCN at reflux; (vi) MeCN–$\mathrm{H_2O}$; (vii) MeCN–$\mathrm{H_2O}$; (viii) MeCN: (ix) MeCN, $\mathrm{HClO_4}$; (x) MeOH, $\mathrm{NaO_2CAr}$.

The presence of a significant metal–metal interaction through the μ-aquo bridge is evidenced from the electrochemical data on **2** and **3**. Although the geometries around the Ru(II) center in **2** and **3** are the same, a considerable shift of the redox potentials is observed between the couples $\mathbf{2'} \rightleftharpoons \mathbf{2'^+}$ and $\mathbf{3'} \rightleftharpoons \mathbf{3'^+}$ or $\mathbf{3'^+} \rightleftharpoons \mathbf{3'^{2+}}$. In fact the $E_{1/2}$ values of the $\mathbf{2'} \rightleftharpoons \mathbf{2'^+}$ couple are inbetween the $E_{1/2}$ values for the two redox couples for **3**. The presence of Cl as the facial ligand on the Ru(III) center in **2** may be responsible for lowering the $E_{1/2}$ value of the oxidation of the Ru(II) center. In absence of any measurable magnetic exchanage phenomena[28] in these low-spin one-electron paramagnetic $t_{2g}{}^5$–$t_{2g}{}^6$ and diamagnetic $t_{2g}{}^6$–$t_{2g}{}^6$ complexes, the electrochemical data are of considerable importance in understanding the metal–metal interactions in **2** and **3**.

Discussion

The reaction pathways leading to the transformation of the diruthenium cores are summarized in Scheme I. In the precursor complex, $\{\mathrm{Ru_2Cl(O_2CAr)_4}\}_x$, the diruthenium(II,III) units are linked by $\mathrm{Cl^-}$ in forming infinite zigzag chains.[18] The formal oxidation state of the metal in the tetracarboxlato-bridged dimeric unit is +2.5, and the Ru–Ru bond order is 2.5 in the $\sigma^2\pi^4\delta^2(\delta^*\pi^*)^3$ ground electronic configuration. When reacted with $\mathrm{PPh_3}$, the polymeric chain undergoes cleavage to form discrete dimeric units. The $\mathrm{PPh_3}$ ligation onto the $\mathrm{Ru_2}$ core might have opened the cage structure whereupon an unusual insertion of a water molecule into the Ru–Ru multiple bond takes place. This leads to a segregation of the oxidation states to $\mathrm{Ru^{III}}$–$\mathrm{Ru^{II}}$ in **2** from the $\mathrm{Ru_2{}^{5+}}$ core of **1**.

The mixed-valence species **2** has a close structural similarity to **3**. The isolation of both diruthenium(II) and diruthenium(III) complexes from reaction 2 indicates the disproportionating nature of the reaction mediated by **2** as given in eq 6. The proposed mechanism is based on the electrochemical data of **2**, showing the presence of two accessible $E_{1/2}$ values for the oxidation as well

---

(27) Nicholson, R. S.; Shain, I. *Anal. Chem.* **1964**, *36*, 706.

(28) Bunker, B. C.; Drago, R. S.; Hendrickson, D. N.; Richman, R. M.; Kessel, S. L. *J. Am. Chem. Soc.* **1978**, *100*, 3805.

$$2\{Ru^{II}Ru^{III}(\mu\text{-}OH_2)(\mu\text{-}O_2CAr)_2{}^{3+}\} \rightarrow \{Ru^{II}{}_2(\mu\text{-}OH_2)(\mu\text{-}O_2CAr)_2{}^{2+}\} + \{Ru^{III}{}_2(\mu\text{-}O)(\mu\text{-}O_2CAr)_2{}^{2+}\} + 2H^+ \quad (6)$$

as for the reduction processes. The **2** → **3** conversion is believed to take place on substitution of Cl by MeCN followed by a one-electron reduction of the core. Similarly, the substitution of Cl^- and MeCN facial ligands in **2** by the $\eta^1\text{-}O_2CAr \rightarrow \eta^2\text{-}O_2CAr$ mode of chelation followed by the $\{Ru^{II}Ru^{III}(\mu\text{-}OH_2)^{5+}\} \rightarrow \{Ru^{III}{}_2(\mu\text{-}O)^{4+}\}$ oxidation of the core leads to the formation of **4**. The third pathway of decomposition of **2** is the substitution of the $\eta^1\text{-}O_2CAr$ ligands by MeCN ligands in forming **5**. The substitution of $\eta^1\text{-}O_2CAr$ facial ligands is expected to make the μ-aquo species unstable in absence of any hydrogen bonds involving these ligands, and μ-oxo core formation takes place on removal of the carboxylic acids, $ArCO_2H$. This process may involve an intermediate (μ-aquo)diruthenium(III) species (eq 4). The removal of hydrogen bonding causes an intramolecular rearrangement of the phosphine ligands which are cis to the μ-oxo group in **4** and **5** as compared to the trans arrangement in the μ-aquo species **2** and **3**. The chelated O_2CAr ligands in **4** undergo a rapid substitution by MeCN on acidification by $HClO_4$ forming **5**. Similarly, **5** converts to **4** on reaction with NaO_2CAr in MeOH.

The reaction chemistry of **1** with PPh_3 observed in a MeCN–H_2O mixture provides valuable information on the earlier reported[10] carbonylation process occurring in alcoholic solvents, $R'CH_2OH$, containing two β-hydrogen atoms (Scheme I). It appears that the reaction proceeds through an intermediate species which is structurally analogous to **2**. A (μ-aquo)diruthenium(II,III) compound with $R'CH_2OH$ bonded to one metal center is likely to be unstable and may lead to the oxidation of the alcohol to aldehyde, from which CO is abstracted to form the ruthenium(II) carbonyl products.

The $\{Ru_2(\mu\text{-}O_2CAr)_4{}^+\} \rightarrow \{Ru_2(\mu\text{-}OH_2)(\mu\text{-}O_2CAr)_2{}^{3+}\}$ core conversion is of interest since it involves two important cases of metal-metal interactions,[25] viz., (i) class III type strong, direct metal–metal interactions and (ii) class II type weak metal–metal interactions, either through space or through a bridging ligand. Compound **2** is expected to serve as a model for triply bridged trapped mixed-valence systems with an $\{M_2(\mu\text{-}OH_2)(\mu\text{-}O_2CR)_2{}^{3+}\}$ core.

In these triply bridged dimetallic systems, the electrochemical results are of significance in understanding the role of facial as well as bridging ligands in tuning and controlling the electronic structure and the stability of the $\{M_2(\mu\text{-}OH_n)(\mu\text{-}O_2CR)_2{}^{m+}\}$ core (n = 0–2; m = 0–4). Considerable interest has been generated in investigating the molecular structure and properties of such a dimeric unit since the discovery of these cores in the active sites of a number of non-heme iron-containing proteins and manganese containing enzymes.[29,30] Oxo-bridged di- and triruthenium phosphine compounds are also useful as homogeneous hydrogenation catalysts.[9] Although the study is extensive on μ-oxo compounds, the chemistry of related μ-aquo/hydroxo species is largely unexplored. The effect of facial ligands in stabilizing the core electronic structure is observed from the cyclic voltammetric data on **2** and **3**. While the presence of a Cl facial ligand in **2** makes the mixed-valence diruthenium(II,III) state stable, the substitution of a π-donor Cl^- by π-acceptor MeCN ligand stabilizes the diruthenium(II) state in **3**. The redox potentials of **2** and **3** show that **2** is more susceptible toward oxidation than **3**.

The observed shift of the redox potentials in **2** and **3** can be compared with the electrochemical data on other known[31-33] (μ-oxo)diruthenium(III) compounds. The $Ru^{III}{}_2/Ru^{III}Ru^{IV}$ couple is known[31,32] to appear at a much higher potential when the facial ligands are pyridine compared to the situation where tridentate triazacyclononane (L) is the facial ligand. Here again the π-acceptor ligand pyridine stabilizes the diruthenium(III) core, while the amine ligand has a tendency to stabilize the diruthenium(III,IV) core.[31]

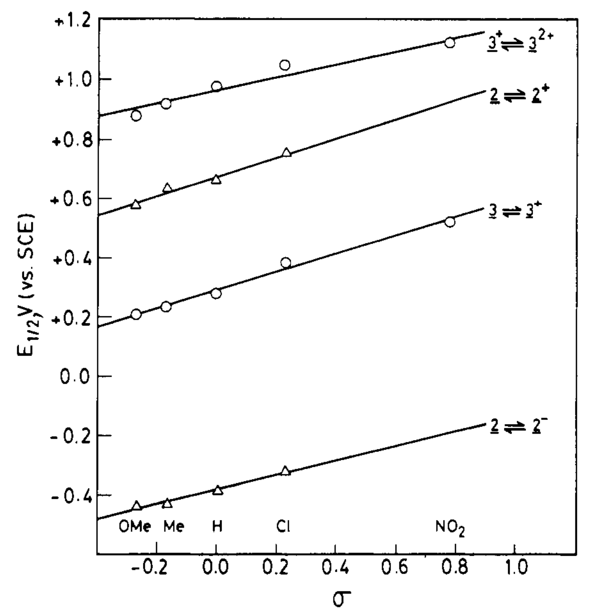

Figure 7. Hammett linear free energy relationships observed for the redox couples in $Ru^{II}Ru^{III}$ complexes **2a**–**2d** (△) and $Ru^{II}{}_2$ complexes **3a**–**3e** (○).

The bridging carboxylato ligands also play an important role in stabilizing the core structure. Using aryl carboxylato bridging ligands, it is possible to see the effect of the para-substituents of the aryl group on the $E_{1/2}$ values for the redox couples in **2** and **3**. Figure 7 shows linear correlations with nearly equal slopes between the $E_{1/2}$ values and the Hammett substitution constants (σ)[34] for the para-substituted benzoic acids. As expected, an electron-withdrawing substituent is found to stabilize the lower oxidation states of the metal.

Compounds **2** and **3** belong to a relatively new "class" of aquo-bridged dimeric species. The structural features of **2** and **3** can be compared with the same in other reported[19-22] compounds (Table VI). In all these compounds the dimeric core is stabilized by strong hydrogen-bonding interactions. The Ru–Ru distances in **2** and **3** are also in accordance with the reported[31] distances in triazacyclononane (L) complexes, $[L_2Ru_2(\mu\text{-}OH)(\mu\text{-}O_2CMe)_2](ClO_4)_3$ (Ru–Ru = 3.47 Å) and $[L_2Ru_2(\mu\text{-}O)(\mu\text{-}O_2CMe)_2](PF_6)_2\cdot 0.5H_2O$ (Ru–Ru = 3.26 Å), showing an increment of +0.21 Å of the Ru–Ru separation on monoprotonation of the μ-oxo bridge. On a second protonation the Ru–Ru separation should further increase to ca. 3.68 Å, which is similar to the distances observed in (μ-aquo)diruthenium compounds.

The unstable nature of **2** toward disproportionation makes these systems comparable to the semimet forms of hemerythrin class of biomolecules and other related model complexes in which the (μ-oxo/hydroxo)bis(μ-carboxylato)diiron(II,III) cores are known[35,36] to be unstable with respect to disproportionation.

Acknowledgment. We are grateful to the Council of Scientific and Industrial Research, New Delhi, for financial support.

Registry No. **1a**, 38832-60-9; **1b**, 116188-30-8; **1c**, 136822-72-5; **1d**, 136822-73-6; **1e**, 136822-74-7; **2a**, 126925-68-6; **2b**, 126925-67-5; **2c**,

---

(29) Lippard, S. J. *Angew. Chem., Int. Ed. Engl.* **1988**, *27*, 344.

(30) Wieghardt, K. *Angew. Chem., Int. Ed. Engl.* **1989**, *28*, 1153.

(31) Neubold, P.; Wieghardt, K.; Nuber, B.; Weiss, J. *Inorg. Chem.* **1989**, *28*, 459.

(32) Sasaki, Y.; Suzuki, M.; Tokiwa, A.; Ebihara, M.; Yamaguchi, T.; Kabuto, C.; Ito, T. *J. Am. Chem. Soc.* **1988**, *110*, 6251.

(33) Llobet, A.; Curry, M. E.; Evans, H. T.; Meyer, T. J. *Inorg. Chem.* **1989**, *28*, 3131.

(34) The values of Hammett σ parameters were taken from: March, J. *Advanced Organic Chemistry, Reactions, Mechanisms and Structure*; McGraw-Hill: New York, 1977; pp 251–259. In $HO_2CC_6H_4$-*p*-X, values for the various X groups are as follows: H, 0.0; OMe, −0.27; Me, −0.17; Cl, +0.23; NO_2, +0.78.

(35) Wilkins, P. C.; Wilkins, R. G. *Coord. Chem. Rev.* **1987**, *79*, 195.

(36) Hartman, J. R.; Rardin, R. L.; Chaudhuri, P.; Pohl, K.; Wieghardt, K.; Nuber, B.; Weiss, J.; Papaefthymiou, G. C.; Frankel, R. B.; Lippard, S. J. *J. Am. Chem. Soc.* **1987**, *109*, 7387.

136822-75-8; **2d**, 136822-76-9; **3a**, 136838-18-1; **3b**, 136838-19-2; **3c**, 136838-20-5; **3d**, 136856-86-5; **3e**, 136838-22-7; $Ru_2Cl(O_2CMe)_4$, 38833-34-0.

Supplementary Material Available: For $Ru_2(OH_2)Cl(MeCN)(O_2CC_6H_4\text{-}p\text{-}OMe)_4(PPh_3)_2$ (**2b**) and $Ru_2(OH_2)(MeCN)_2(O_2CC_6H_4\text{-}p\text{-}NO_2)_4(PPh_3)_2\cdot 1.5CH_2Cl_2$ (**3e**), details of crystal structure determination, tables of crystal data, positional and isotropic thermal parameters, anisotropic thermal parameters, and bond lengths and angles (22 pages); tables of observed and calculated structure factors for **2b** and **3e** (70 pages). Ordering information is given on any current masthead page.

Contribution from the Department of Chemistry,
Purdue University, West Lafayette, Indiana 47907

Reactions of the Polyhydride Complex $ReH_7(PPh_3)_2$ with Hydroxypyridine and Mercaptopyridine Ligands. Formation of Hydrido Complexes of Rhenium(III), Rhenium(IV), and Rhenium(V) and the Characterization of Eight-Coordinate Isomers in the Solid State and in Solution

Malee Leeaphon, Phillip E. Fanwick, and Richard A. Walton*

Received August 30, 1991

The reactions of the heptahydride complex $ReH_7(PPh_3)_2$ with 2-hydroxypyridine (Hhp), 2-mercaptopyridine (Hmp) and 2-hydroxy-6-methylpyridine (Hmhp) in acetone afford the diamagnetic seven-coordinate complexes $ReH(L)_2(PPh_3)_2$ (L = hp, mp, mhp), which can be oxidized by one electron when treated with $[(\eta^5\text{-}C_5H_5)_2Fe]PF_6$ in dichloromethane to give paramagnetic $[ReH(L)_2(PPh_3)_2]PF_6$. These are rare examples of mononuclear rhenium(IV) hydrides. While the 17-electron mp derivative is stable in solution, the related hp and mhp complexes decompose (probably by a disproportionation mechanism) to give the dihydrides $[ReH_2(L)_2(PPh_3)_2]PF_6$ as the major products. In these latter reactions small quantities of the seven-coordinate oxorhenium(V) complexes $[ReO(L)_2(PPh_3)_2]PF_6$ can also be isolated. The crystal structure of $[ReO(mhp)_2(PPh_3)_2]PF_6\cdot C_2H_4Cl_2$ (**4**) shows that it is based upon a distorted pentagonal bipyramid with a P–Re–P angle of ca. 169° and with the oxo ligand occupying a position within the pentagonal plane. The diamagnetic dihydrido species $[ReH_2(L)_2(PPh_3)_2]PF_6$ are also formed in all cases upon treatment of $ReH(L)_2(PPh_3)_2$ with HPF_6 in dichloromethane. The mp derivative is unstable and converts to $[ReH(mp)_2(PPh_3)_2]PF_6$ with loss of H_2. The hp complex $[ReH_2(hp)_2(PPh_3)_2]PF_6$ is stable both in the solid state and in solution, and is identical in all respects with the form of this complex that is isolated from the decomposition of $[ReH(hp)_2(PPh_3)_2]PF_6$. On the other hand, the complex of composition $[ReH_2(mhp)_2(PPh_3)_2]PF_6$ exists in two geometric isomeric forms. The product that is obtained upon decomposition of the 17-electron complex $[ReH(mhp)_2(PPh_3)_2]PF_6$ is denoted as the cis isomer and is the more thermodynamically stable form of the two. The trans isomer is the form that is obtained by protonation of neutral $ReH(mhp)_2(PPh_3)_2$. Both isomers have structures that are based upon distorted dodecahedral geometries with the hydrogen and oxygen atoms at the A sites and the nitrogen and phosphorus atoms at the B sites of an MA_4B_4 dodecahedron. Crystal structures on one form of the trans isomer and two different crystalline forms of the cis isomer have been determined, viz., *trans*-$[ReH_2(mhp)_2(PPh_3)_2]PF_6\cdot C_2H_4Cl_2$ (**1**), *cis*-$[ReH_2(mhp)_2(PPh_3)_2]PF_6\cdot (CH_3)_2CO$ (**2**), and *cis*-$[ReH_2(mhp)_2(PPh_3)_2]PF_6\cdot 0.5C_2H_4Cl_2$ (**3**). Each isomer appears to be a classical dihydride. They both have an independent existence in solution although the trans isomer converts very slowly to the cis isomer. This is the first time that eight-coordinate geometric isomers which are stable both in the solid state and in solution have been structurally characterized. These two isomers, as well as $[ReH_2(hp)_2(PPh_3)_2]PF_6$, are easily deprotonated by NEt_3 and/or DBU to re-form the parent neutral monohydrides $ReH(L)_2(PPh_3)_2$. Crystal data for **1** (−62 °C): triclinic space group $P\bar{1}$ (No. 2), $a = 13.382$ (2) Å, $b = 13.723$ (2) Å, $c = 15.593$ (2) Å, $\alpha = 107.06$ (1)°, $\beta = 96.54$ (1)°, $\gamma = 114.05$ (1)°, $V = 2408$ (2) Å^3, $Z = 2$. Crystal data for **2** (−96 °C): orthorhombic space group *Pbca* (No. 61), $a = 19.292$ (2) Å, $b = 22.399$ (2) Å, $c = 22.314$ (2) Å, $\alpha = \beta = \gamma = 90°$, $V = 9642$ (3) Å^3, $Z = 8$. Crystal data for **3** (+20 °C): triclinic space group $P\bar{1}$ (No. 2), $a = 15.075$ (4) Å, $b = 18.640$ (4) Å, $c = 20.662$ (6) Å, $\alpha = 114.53$ (1)°, $\beta = 100.44$ (2)°, $\gamma = 98.40$ (2)°, $V = 5033$ (5) Å^3, $Z = 4$. Crystal data for **4** (+20 °C): monoclinic space group $P2_1/c$ (No. 14), $a = 11.794$ (2) Å, $b = 14.168$ (1) Å, $c = 31.359$ (5) Å, $\beta = 110.776$ (6)°, $V = 4899$ (2) Å^3, $Z = 4$. All structures were refined by full-matrix least-squares methods to the following values of R (R_w given in parentheses) for the stated number of data with $I > 3.0\sigma(I)$: **1**, 0.023 (0.030), 5706 data; **2**, 0.036 (0.049), 4536 data; **3**, 0.059 (0.081), 8473 data; **4**, 0.041 (0.049), 4525 data.

Introduction

Transition-metal polyhydrides are well-known for exhibiting fluxionally.[1] This is especially true in the case of rhenium polyhydrides, for which a greater variety of such complexes exist than for any other transition metal.[2] Accordingly, one would not normally expect geometric isomerism to be encountered in solutions of such species, especially for those compounds that possess coordination numbers greater than 6. Indeed, the phenomenon of geometric isomerism is rarely encountered in the case of eight-coordination, and the definitive structural characterization of such isomers has only been reported in rare instances for solid-state species[3,4] and in no instance in solution. Nonetheless, while the stabilization of eight-coordinate geometric isomers has long been recognized as a challenging and somewhat daunting task,[5] a series of important studies in the period 1977–1985 by Archer and Donahue[6] on tungsten(IV) complexes that contained four bidentate or two tetradentate donors showed that eight-co-

---

(1) See, for example: Hlatky, G. G.; Crabtree, R. H. *Coord. Chem. Rev.* **1985**, *65*, 1 and references contained therein.

(2) Conner, K. A.; Walton, R. A. In *Comprehensive Coordination Chemistry*; Pergamon: Oxford, England, 1987; Chapter 43, pp 125–213.

(3) (a) Sen, A.; Chebolu, V.; Rheingold, A. L. *Inorg. Chem.* **1987**, *26*, 1821. (b) Chebolu, V.; Whittle, R. R.; Sen, A. *Inorg. Chem.* **1985**, *24*, 3082. (c) Fanfani, L.; Nunzi, A.; Zanazi, P. F.; Zanzari, A. R. *Acta Crystallogr., Sect. B: Struct. Crystallogr. Cryst. Chem.* **1972**, *28*, 1298.

(4) Isomers can also be obtained by varying a counterion as, for example, in the case of salts of the $[Nb(C_2O_4)_4]^{4-}$ anion, viz., $K_2(H_3NCH_2CH_2NH_3)[Nb(C_2O_4)_4]\cdot 4H_2O$ and $K_4[Nb(C_2O_4)_4]\cdot 3H_2O$. See: Cotton, F. A.; Diebold, M. P.; Roth, W. J. *Inorg. Chem.* **1987**, *26*, 2889.

(5) Lippard, S. J. *Prog. Inorg. Chem.* **1967**, *8*, 109.

(6) (a) Donahue, C. J.; Archer, R. D. *J. Am. Chem. Soc.* **1977**, *99*, 6613. (b) Donahue, C. J.; Clark-Motia, D.; Harvey, M. E. *Inorg. Chem.* **1985**, *24*, 801. (c) Donahue, C. J.;Kosinski, E. C.; Martin, V. A. *Inorg. Chem.* **1985**, *24*, 1997.

0020-1669/91/1330-4986$02.50/0